Laboratory measurement of dispersion and attenuation in the seismic frequency

Qi Huang, De-hua Han, Hui Li,*
Rock Physics Laboratory, University of Houston

Summary

We have continuously made progress in dispersion/attenuation study in laboratory measurement. We calibrated the lab low frequency measurement system for velocity dispersion and wave attenuation. And we test the system by measuring some dry samples, which shows our system can produce repeatable and reasonable result. Currently, we're conducting the system calibration with confining pressure and pore pressure under different saturation.

Introduction

Dispersion is the variation of velocity with frequency, whereas attenuation is the loss of wave amplitudes with distance. The details in dispersion and attenuation depend on the rock microstructure, larger-scale geology, and fluids. In past decade, we saw continuous progress in theoretical study of seismic wave attenuation and dispersion in reservoir rocks. (Muller 2010, Tang 2011, Gurevich 2011).

There are three reasons that a low frequency measurement system is essential to the study of velocity dispersion and attenuation. First, the traditional laboratory measurements of the velocities in reservoir rocks are conducted in MHz frequency range. Sonic well logs are in 10 kHz and surface seismic in several Hz to hundred Hz. Low fequency mensurement can help integrate all kinds of data satsifying today's challenging exploration. Second, it can verify various dispersion and attenuation mechanisms and proposed model, which can expand the understanding of rock properties. Also, recent theoretical works reveal that the dispersion and attenuation in reservoir rock is closely related to the interaction between pore fluid and rock frame. It's neccesary to collect sufficient lab test results to establish some robust relationships that can serve as fluid indicator.

Progress in laboratory measurement of the dispersion and attenuation in seismic frequency is still in primary stage in terms of quality of the data produced. This is due to two factors. First, different techniques cover different frequency ranges, none of them can fully cover seismic to ultrasonic range. Second, in the most used method, force-deformation method, S/N ratio is too small and thus data is not stable and repeatable. Meanwhile, lack of calibration on system errors prevent us from being confident with the data.

Our recent effort on improving the quality data of low measurement includes two corresponding two aspects: enhancement of S/N signal and result verification, which also can help extend the measurement frequency range. And testing measurements show very good repeatability.

Low frequency measurement system and principles

From Fig.1, the system consists of three parts, platen, measurement column and PZT actuator. The hydraulic pressure on the upper platen can help make the whole column tighter and thus stress on the column is uniform. The PZT actuator vibrate as a sine function with different frequency. It can provide a much higher force than a coil-magnet pair vibrator and the strain amplitude can easily reach 10^{-7} and even 10^{-6}. Furthermore, the standard is repeatedly used, which can make data from different sample comparable. On the other hand, by using different standards, we can compare the data of same sample.

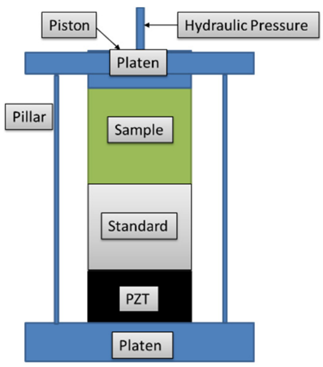

Figure 1. The schematic figure of low frequency measurement system

The standard core plug is stacked with the rock sample, and the strain of the standard and sample core are measured. Since the standard and rock sample are subject to the same stress field, the ratio of their strains should be equal to the reverse ratio of their Young's modulus. In our system, solid Alumimum core and hollow Titanium core are used as the standard, whose Young's modulus are respectively 69 GPa and 17.8 GPa. Applying the vertical stress with specified frequency on the measurement column, the vertical strain can be used to calculate the Young's modulus of the rock core plug.

$$E_{sample} = E_{std} * \left(\frac{\varepsilon_{std\_V}}{\varepsilon_{sample\_V}}\right)$$

The horizontal strain of the sample are recorded at the same time, and Poisson' ratio can be calculated by,

$$\nu = -\frac{\varepsilon_{sample\_H}}{\varepsilon_{sample\_V}}$$

Also, Aluminum and Titanium can be viewed as pure elastic medium, so the phase of its strain should be equal to the

DOI http://dx.doi.org/10.1190/segam2015-5909141.1

phase of the stress. Then we can use the phase difference θ between standard and sample to calculate the inverse quality factor of the rock sample. (White, 1983; Paffenholz and Burkhardt, 1989)

$$Q = 1/\tan(\theta)$$

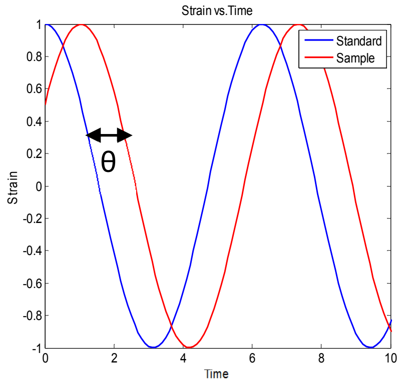

Figure 2. The schematic figure of phase difference between standard and sample

The next important thing is to install stain gauges on both sample and standard to record the strain at each frequency point. Wheastone bridge becomes our choice. In the Fig. 3, it consists of two resistors and two strain gauges (azimuth angle 180 degree) with the nominal resistance (at zero strain) equal to the standard resistors. The relationship between strain and output voltage signal, which is recorded in our low frequency system, is

$$V_{out} = V_{ex} * \varepsilon * GF * AF/2$$

Where V_{out} is output voltage, V_{ex} is excitation voltage, ε is strain, GF is gauge factor, and AF is amplification factor. In the right hand, except for stain, all others are constant in our system, so the stain is proportional to the output voltage, and the stain ratio can be represented by output voltage ratio. In our system, V_{ex} is 12V, GF is 130 and AF is 200, so the output signal is 156000 times as the orginal strain.

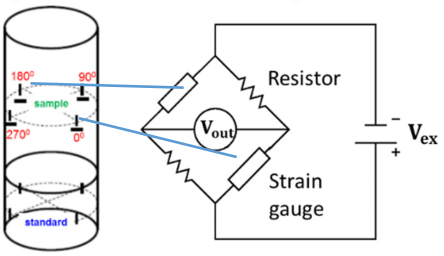

Figure 3. Stain gauge arrangement and Wheastone bridge

As shown in the Fig 4, all 6 channels are displayed, Ch1 and Ch2 are vertical stain signal of the sample, Ch3 and Ch4 are horizontal stain signal of the sample and Ch5 and Ch6 are vertical stain signal of the standard. In reality, the strain ratio is obvious but the phase difference is very small and difficult to extract from data. By using virtual lock-in amplifier, this problem was solved.

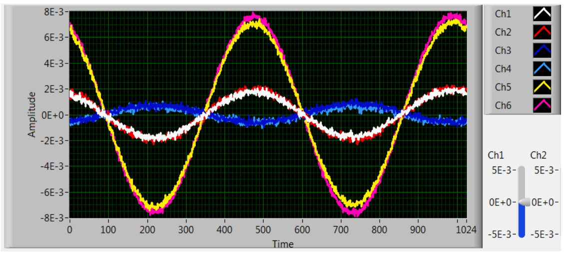

Figure 4. Strain waveform at Frequency 200Hz

Measurement results and analysis

Eight samples are measured to test our low frequency measurement system. In all the samples, there are one Aluminum sample, one PEEK sample, one Lucite sample, one Berea sandstone sample, three Mancos shale samples and one Jimsar shale sample. All the samples are vacuumed for 48 hours before measurement. No confining pressure and pore pressure is applied. Plus, two standards made of Aluminum and Titanium are used to measure the samples' Young's modulus and Poission's ratio. Frequency points range from 2Hz to 800Hz covering the whole seismic frequency domain.

First we measured Young's modulus of the Aluminum sample(69 GPa) to calibrate the system. In the Fig.5, the result from both Aluminum and Titanium standards match the expectation, which shows the stablity and reliablity of our low frequency mesurement system.

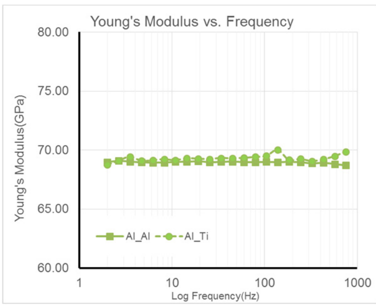

Figure 5. Young's modulus of Aluminum

The second sample is PEEK, namely Polyether ether ketone, which is treated as elastic in engineering applications. As shown in the Fig.6 we can see the Young's modulus of PEEK is almost constant as frequency increases; but interestingly its quality factor goes down with the increase

DOI http://dx.doi.org/10.1190/segam2015-5909141.1

of frequency. Lucite's Young's modulus is in the Fig.7, which increases by 30% as frequency increases from 2Hz-800Hz. This is because Lucite is viscous, which is reflected by its low quality factor.

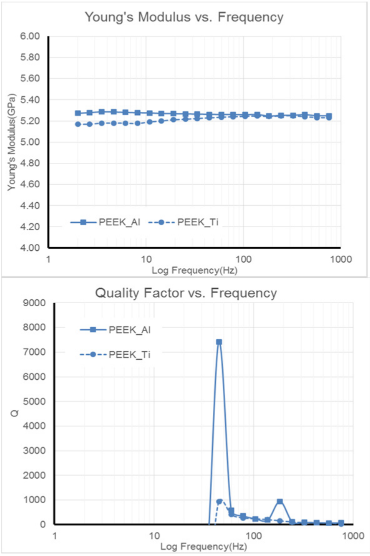

Figure 6. Young's modulus and quality factor of PEEK sample

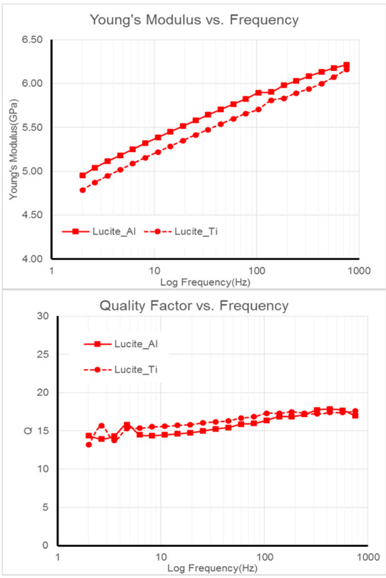

Figure 7. Young's modulus and quality factor of Lucite sample

As shown in the Fig.8, the Young's modulus of Berea sandstone sample has nearly no dispersion but its quality factor goes up as frequency increases.

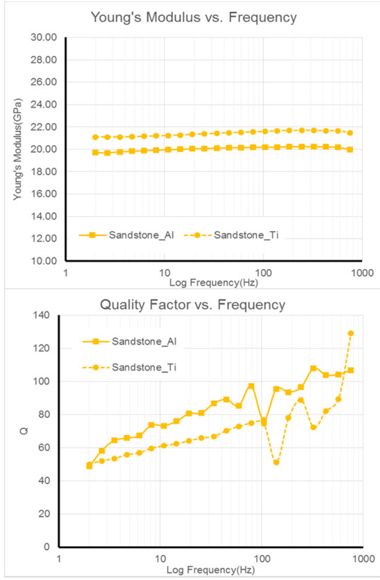

Figure 8. Young's modulus and quality factor of Berea sandstone sample

Three shale samples from Mancos are measured. V1 is a vertical sample and H2 and H3 are horizontal samples. In the Fig.9, H2 and H3 have no dispersion but V1 has a little dispersion, which is corresponding with the quality factor result. H2 and H3 have higher quality factors but V1 has a lower one less than 50.

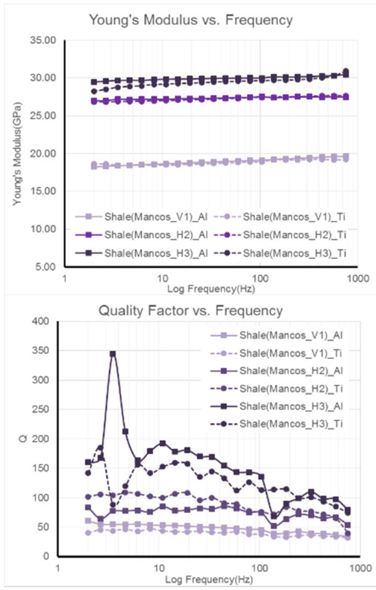

Figure 9. Young's modulus and quality factor of Mancos Shale sample

From Fig.10, we can see an obvious increase of Young's modulus of Xinjiang shale sample and its quality factor is very low less than 30. One possible explanation is the effect of organic matter inside the rock. Since we have its density, we can translate the Young's modulus and Poisson's ratio into P-wave and S-wave velocity. Also, we measured its ultrasonic velocity. From the Fig. 11, the velocity dispersion is very large and the trend of low frequency measurement is consistent with the ultrasonic data.

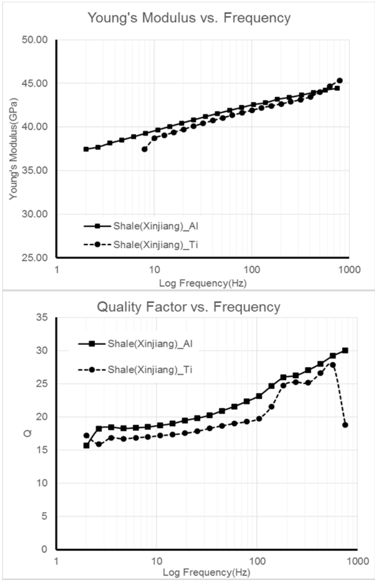

Figure 10. Young's modulus and quality factor of Xinjiang shale

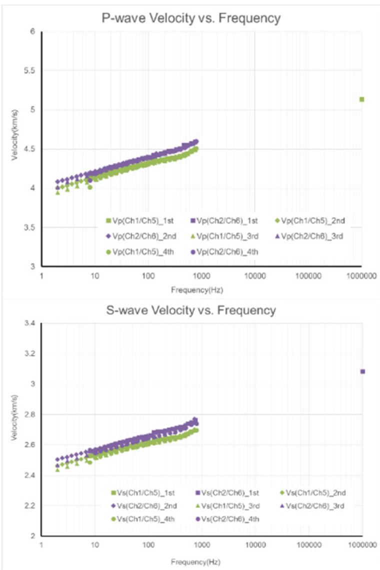

Figure 11. Velocity dispersion of Xinjiang shale sample

The last figure is the Poisson's ratio of five samples, since there is no horizontal strain gauge on Aluminum sample, PEEK sample and sandstone sample. We can notice that the Poisson's ratio changes little with frequency.

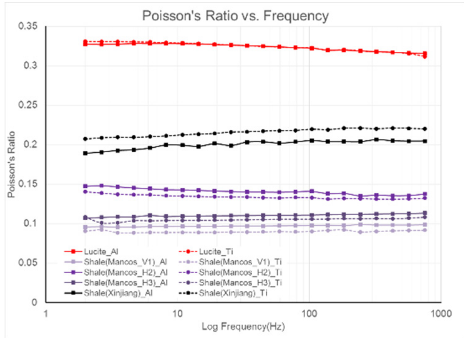

Figure 12. Poisson's ratio of Lucite, Mancos shale and Xinjiang shale sample

Conclusion

To sum up, large strees by PZT atuator can increase the strain amplitude; output signal can be amplifed 156000 times as orginal strain with application of high-gauge-factor strain gauge and high-amplication amplifier. The final S/N ratio is essentially improved. Also, the dispersion and attenuation of rock sample can be extracted under the low S/N ratio condition by virtual lock-in amplifier and low frequency measurement software. Meanwhile, the introduction of repeatable standard, we can verify the low frequency measurement result and repeat the measurement to acquire a more accurate result. In future, we'll conduct low frequency measurement with applying confining pressure and pore pressure under different saturation.

Acknowledgement

Frist of all, I want to express my sincere thanks to Fluid/DHI Consortium for long term financial support. I would also like to thank Dr. Yao for building the low frequency measurement. Plus, I'm deeply thankful for unselfish helps and supports from my advisor Dr. Han. At last, I want to acknowledge my colleagues, Fuyong Yan, Hui Li, and Xuan Qin for discussion and refreshed ideas.

DOI http://dx.doi.org/10.1190/segam2015-5909141.1

EDITED REFERENCES

Note: This reference list is a copyedited version of the reference list submitted by the author. Reference lists for the 2015 SEG Technical Program Expanded Abstracts have been copyedited so that references provided with the online metadata for each paper will achieve a high degree of linking to cited sources that appear on the Web.

REFERENCES

Adam, L., M. L. Batzle, K. T. Lewallen, and K. van Wijk, 2009, Seismic wave attenuation in carbonates: Journal of Geophysical Research, **114**, B6, B06208. http://dx.doi.org/10.1029/2008JB005890.

Batzle, M. L., D. H. Han, and R. Hofmann, 2006, Fluid mobility and frequency-dependent seismic velocity — Direct measurements: Geophysics, **71**, no. 1, N1–N9. http://dx.doi.org/10.1190/1.2159053.

Czichos, H., T. Saito, and L. Smith, 2006, Springer handbook of materials measurement methods: Springer. http://dx.doi.org/10.1007/978-3-540-30300-8.

Das, A., 2010, The viscoelastic properties of heavy-oil saturated rocks: Ph.D. dissertation, Colorado School of Mines.

Domenico, S. N., 1976, Effect of brine-gas mixture on velocity in an unconsolidated sand reservoir: Geophysics, **41**, 882–894. http://dx.doi.org/10.1190/1.1440670.

Gautam, K., 2003, Fluid effects on attenuation and dispersion of elastic waves: M.Sc. thesis, Colorado School of Mines.

Gist, G. A., 1994, Interpreting laboratory velocity measurements in partially gas-saturated rocks: Geophysics, **59**, 1100–1109. http://dx.doi.org/10.1190/1.1443666.

Gregory, A. R., 1976, Fluid saturation effects on dynamic elastic properties of sedimentary rocks: Geophysics, **41**, 895–921. http://dx.doi.org/10.1190/1.1440671.

Gurevich, B., D. Makarynska, and O. de Paula, 2011, Bounds for seismic dispersion and attenuation in poroelastic rocks: 81st Annual International Meeting, SEG, Expanded Abstracts, 2155–2160.

Liu, H. P., D. L. Anderson, and H. Kanamori, 1976, Velocity dispersion due to anelasticity: Implications for seismology and mantle composition: Geophysical Journal of the Royal Astronomical Society, **47**, no. 1, 41–58. http://dx.doi.org/10.1111/j.1365-246X.1976.tb01261.x.

Liu, H., and L. Peselnick, 1983, Investigation of internal friction in fused quartz, steel, Plexiglas, and Westerly Granite from 0.01 to 1.00 Hertz: Journal of Geophysical Research, **88**, B3, 2367–2379. http://dx.doi.org/10.1029/JB088iB03p02367.

McKavanagh, B., and F. D. Stacey, 1974, Mechanical hysteresis in rocks at low strain amplitudes and seismic frequencies: Physics of the Earth and Planetary Interiors, **8**, no. 3, 246–250. http://dx.doi.org/10.1016/0031-9201(74)90091-0.

Muller, T. M., B. Gurevich, and M. Lebedev, 2010, Seismic wave attenuation and dispersion resulting from wave-induced flow in porous rocks — A review: Geophysics, **75**, no. 5, 75A147–75A164.

Tang, X. M., 2011, A unified theory for elastic wave propagation through porous media containing cracks — An extension of Biot’s poroelastic wave theory: Science China: Earth Science, **54**, no. 9, 1441–1452.

Thomsen, L.,1985 Geophysics, Biot-consistent elastic moduli of porous rocks: Low-frequency limit: Geophysics, **50**, 2797–2807

Zhang, S., F. D. Maestra, N. Combaret, R. Klimentidis, P. Barthelemy, R. Albou, D. Lichau, and D. Bernard, 2011, The analysis and simulation of rock properties using FIB-SEM and virtual material studio: NAFEMS World Congress.